Carcinoma classification from breast histopathology images using a multi level spatial fusion mechanism of deep convolutional features from differently stain normalized patches

Ritabrata Sanyal[1], Kunal Chakrabarty[2] Gummi Deepak Reddy[3], and Vinayak Sengupta[4]

[1] Kalyani Government Engineering College, West Bengal, India
sritabrata@gmail.com
[2] Kalyani Government Engineering College, West Bengal, India
kunalchakrabarty@gmail.com
[3] Jawaharlal Nehru Technological University, Hyderabad, India
gummideepak@gmail.com
[4] BITS Pilani, Dubai, UAE
vinayak.sengupta@gmail.com

Abstract. Breast cancer is one of the leading causes behind death of women worldwide. Core needle biopsy of breast tissue, followed by analysis of the breast histopathological image is one of the most widely used breast cancer diagnosis techniques today. Deep learning pipelines involving a single stain normalization of the raw histology images, followed by patch extraction and CNN based patch wise classification methods with integration of patch wise results by majority voting for image wise classification, have already been proposed in literature. This paper presents a novel architecture, based on spatial fusion of features of two different stain normalizations of the an input patch. The underlying mechanism of stain normalization algorithms being different, they bring forth different salient features of a histopathology image. This will aid a CNN network learn better representations, which will not be possible had only one stain normalization method been used like previous methods. The final feature representation of a patch is rich and multilevel, that is it takes both low level (finer features) and high level (coarser features) features into account. Finally, the feature vector extracted from every patch is fed to a Bidirectional Long Short Term Memory (BLSTM) network for image wise classification, to exploit long term and short term contextual information between neighbourhood patches. Experiments reveal that our model achieved a 87.75% and 97.5% for patch and image wise classification respectively on the ICIAR 2018 breast histopathological images dataset, thereby outperforming other state of the art methods to the best of our knowledge.

Keywords: Breast cancer · Histopathology analysis · Deep Learning · Convolutional Neural Network (CNN) · Long Short Term Memory (LSTM)

1 Introduction

Breast Cancer is a global health problem accounting for the second most cancer deaths in women worldwide. The microscopic analysis of hematoxylin and eosin(H & E) stained histopathological images is the most widely used method for it's diagnosis and early detection. However, manual analysis of these images suffers from various shortcomings including pathologists' bias and diagnostic inconsistencies, thus, necessitating the development of automated breast cancer detection mechanisms.

The recent advancements of Deep Learning methods in various image classification tasks has inspired scholars to use them for classification of medical images. Spanhol et al. [14] released a breast cancer histopathological patches dataset, captured at different magnifications, based on which they used a Convolutional Neural Network trained on Imagenet for classifying breast cancer type from the histopathological images. Araujo et al. [1] first considered the problem of high resolution breast histopathology image classification, and proposed a pipeline comprising of Macenko [9] stain normalization, patch extraction and classifying each patch with a AlexNet CNN. Roy et al. [12] also used Macenko [9] stain normalization and proposed a custom CNN architecture for patch based classification. Vang et al. [17] used both Vahadane [16] and Macenko [9] stain normalized patches to train an Inceptionv3 [15] network for patch wise classification. Then they ensembled the predictions from Vahadane [16] and Macenko [9] stained patches trained CNNs, to obtain the final classification result.

A common trait among the deep learning based methods heretofore is the use of a single stain normalization method on the raw histopathological images, followed by dividing the image into patches, classifying each patch and finally integration of patch wise classification results, to obtain image wise predictions. Stain normalization methods help reduce the undesirable colour variations that may arise from H & E staining on histopathological images.Various such stain normalization procedures have different underlying principles to mitigate such colour variations. However, we observed that various stain normalization methods bring forth different salient features in the histology images. That is, the use of only one stain normalization method therefore is somewhat inimical to the network's ability to learn global features and generalize well. As mentioned earlier, Vang et al. [17] used two stain normalization methods for patch wise classification, but they trained their networks independently and ensembled the predictions. However, this process fails to fuse the features of two stain maps of a patch spatially to output a single representation incorporating features of both the stained patches. This can be only obtained with joint training, so that during a single forward pass through the entire network, features from both the stain normalized patches contribute to the final output. We hypothesize that a rich spatial feature fusion of the feature map generated by two stain normalization methods will give better results than using a single stain normalization method. The two stain normalized patches will bring forth different prominent regions of the input patch.

To that end we propose a novel architecture, that uses two different stain normalization methods on patchwise training of histopathological images as suggested in Macenko et al. [9] and Vahadane et al. [16]. We effectively combine features from different convolutional layers to get an accurate feature representations of these normalization procedures to obtain a richer multilevel representation for the histopathological image patch. We then extract a feature vector representation of the patch. The patches of the image are then input to a bidirectional long short-term memory(LSTM) [6] module and the class label of the image is predicted.

2 Dataset

Our work uses the Breast Cancer Histology Challenge (BACH) 2018 dataset [2] which was hosted as part of the ICIAR 2018 conference, consisting of high resolution H&E stained breast histology images. These RGB images are of size 2048x1536 pixels with each pixel covering 0.42 µm x 0.42 µm of tissue area. Each image is annotated into 4 different classes, namely Benign, Normal, Insitu Carcinoma and Invasive Carcinoma. Figure 1 shows sample images from each category. There are 100 images in each category.

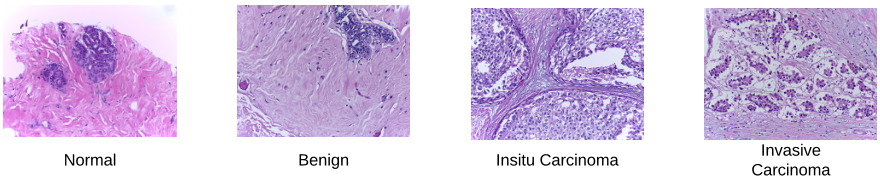

Fig. 1: Sample images with their corresponding classes from the ICIAR 2018 dataset

3 Methodology

In this section we will describe our model architecture. At first, two stain maps of a breast histology image is computed by the Vahadane [16] and Macenko [9] stain normalization algorithm respectively. Each of the stain normalized images are divided into 35, 512×512 patches with 50% overlap, generating two patch wise datasets—— one of Vahadane type and the other Macenko type. Two pretrained VGG19 [13] networks are then fine-tuned on the two patch datasets, for feature extraction of each type of stain images. After this, higher and lower level feature maps, extracted from the 2 VGG19 nets, are fed to the Stain-feature Fusion Network, to compute a rich representation of a patch, and finally classify

the patch. For image level classification, the rich patch representations are fed to a BLSTM network, to maintain both long and short term associations between various patches. The methods are elaborated as follows:

3.1 Preprocessing

Accurate preprocessing is of histology images is of paramount importance towards development of a rigorous prediction model. H & E stained images suffer from unwanted color shifts due to the variations in slide scanners and level of stain absorption. Other variations like difference in stain reactivity from different manufacturers may contribute to this as well . These shifts in color may introduce a bias in our model prohibiting it from generalizing well. So to normalize this we use the methods suggested by Vahadane et al. [16] and Macenko et al. [9]. Vahadane et al. [16] uses a sparse non-negative matrix factorization based technique for normalizing stained patches whereas Macenko et al. [9] proposed a method based on normalizing the colors in the input RGB image to optical density (OD). It is then followed by applying Singular Value Decomposition on the optical density vectors, which effectively restores useful features by projecting the image in a 2-D plane and using the vectors with a high degree of variance. In Figure 2, we can see the results of each stain normalization method on a sample image.

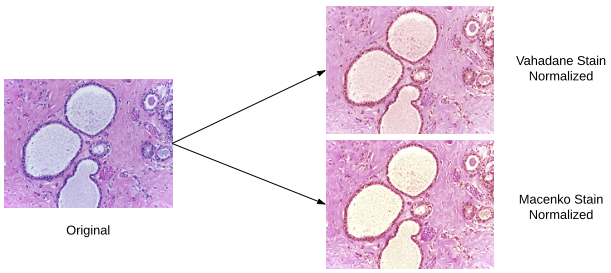

Fig. 2: The two types of stain normalization on an image

3.2 Patch Extraction

The images in our dataset are of a very high resolution (2048 x 1536). Deep Learning models trained on such large spatial dimensions tend to suffer from over-fitting and the paucity of images in the dataset exacerbates the problem. To rectify this, we extract patches from the images. This both helps us process these large images and also acts as a data augmentation technique.

Patches of dimensions 512 x 512 with 50% overlap are extracted from the original images in a sliding window fashion. We have empirically observed these dimensions to be yielding the best results.

3.3 Patch wise classification

Our Patch wise classifier consists of two component networks, namely the Stain Feature Extraction Network (SFEN) and the Stain Feature Fusion Network (SFFN). SFEN deals with finetuning two CNNs on the two stain normalized patch datasets, and thus extracting higher and lower level features. SFFN fuses the high and low level features extracted from each CNN, to effectively combine spatial information of two stain normalized versions of the same input patch. Figure 3 is a visual representation of the same.

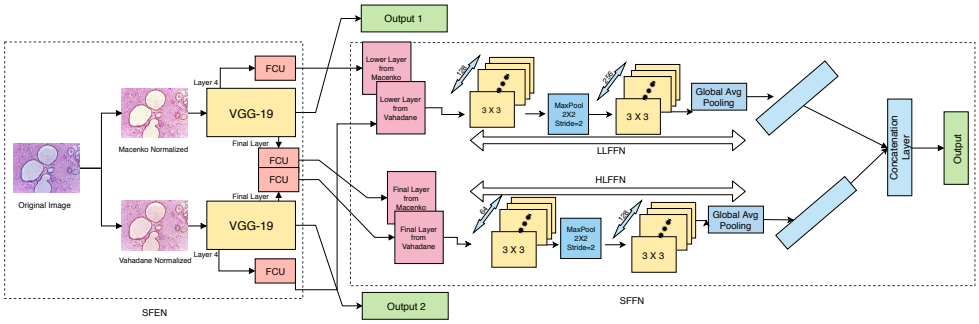

Fig. 3: The patch-wise classification pipeline. Output 1 and 2 represents the softmax outputs of the backbone VGG-19 networks. Output 3 is the softmax output of the SFFN.

Stain Feature Extraction Network (SFEN) SFEN consists of two independent backbone CNN networks, each responsible for learning features from a Vahadane and Macenko stained normalized input patch, respectively, and a novel Feature Control Unit (FCU) as shown in Figure 4, for extracting high and level features from the two backbone CNNs. The backbone networks are two VGG19 networks [13], pretrained on the Imagenet [3] dataset, which we finetune on both of the stain normalized patch datasets . Finetuning strategy is chosen, mainly due to the paucity of our dataset and that fine-tuning helps the CNN to learn target task specific features, yet with considerably less training data than it would be required if the CNNs were trained from scratch. After fine-tuning, we extract both high and low level features from both CNNs. It is essential to make up for the coarser convolutional features with more receptive fields.Retaining fine information like edges, corners, curves, local intensity variations which are extracted by the lower layers, we extract both high and low level features from both the CNNs. It is to be noted that, the rich multilevel features extracted by the backbone nets must spatially correspond to each other, for the SFFN network to construct coherent meaning of the input patch——that is, any spatial location of a low level feature map output of the backbone net trained on

Vahadane [16] stained patches must correspond to the same location in the low level feature map output of the backbone net trained on Macenko [9] stained patches. To that end, we propose a novel rich feature extraction mechanism, namely the Feature Control Unit (FCU). A FCU takes as input the feature map output (a $3-D$ tensor) of a certain convolutional layer of a backbone CNN, and outputs a single feature map (a $2-D$ matrix). The FCU consists of a stack of 512, 1×1 [8] convolutional kernels for increasing the non-linearity of the decision function without influencing the receptive fields of the convolutional layer of the backbone network, which is followed by channel-wise pooling with a single 1×1 kernel for projecting the output from the previous layer into a space of lower dimensionality ($2-D$ from $3-D$). Rectified Linear Unit (ReLU) [4] non-linearity is used in every layer of the FCU. The maps are channel wise pooled, as it would decrease the complexity of feature combination of the SFFN network, while preserving the spatial correspondence between maps extracted from both the CNNs. An architecture like FCU is chosen mainly because the two backbone CNNs and the feature fusion net (SFFN) are trained independently, so the features extracted by the backbone nets are not augmented during back-propagation through the SFFN network——which is detrimental for the SFFN to effectively learn the feature fusion mechanism. Hence we add another layer of non-linearity on top of the backbone CNN extracted feature maps, thereby regulating/controlling the nature of features to flow into the SFFN network. To extract lower level features, we take the 256×256 feature map output from the fourth convolutional layer of each backbone VGG19 net and feed it to a FCU. The procedure is same for extracting high level features, except we use the last convolutional layer 32×32 feature map output.

Stain Feature Fusion Network (SFFN) After the high and low level feature maps are extracted by the FCU of the SFEN network, the high level maps of both the backbone nets are paired, and same is done with the low level maps, which are then fed to the SFFN network. The fusion strategy entails in effective combination of high level features of both stain normalized patches and low level features of the same. This is done to incorporate high and low level features of both Vahadane [16] and Macenko [9] stain normalized versions, to generate a rich, multilevel feature representation of an input patch. SFFN network consists of two parallel networks, one for combining high level features, namely High Level Feature Fusion Net (HLFFN), and the other for combining low level features, namely Low Level Feature Fusion Net (LLFFN), as described below:

- **LLFFN :** This network accepts two 256×256 lower level feature maps, and fuses them to obtain a vector representation. This aids in incorporating features of any spatial region, which are accentuated by either or both the Vahadane [16] and Macenko [9] stain normalized versions of an input patch. LLFFN consists of two convolution layers followed by a Global Average Pooling (GAP) layer [8]. The first convolutional layer has 128, 3×3 kernel filters, followed by a Max-Pooling layer to reduce the spatial dimensions of the feature map. The second convolutional layer has 256, 3×3 kernel filters,

followed by the GAP layer to output a 256 dimensional feature vector. The GAP layer carries out feature pooling on the output feature map, hence helps in dimensionality reduction, compared to flattening the map as a vector.

– **HLFFN :** HLFFN accepts two 32×32 feature maps and outputs a 128 dimensional feature vector, representative of the high level features of an input patch. The topology of this network is almost same as LLFFN except for a few differences. The first convolutional layer has 64, 3×3 kernel filters, and the second one has 128, 3×3 kernel filters.

All the convolutional layers of the LLFFN and HLFFN nets have ReLU non-linearity. The low and high level feature vectors, output by the LLFFN and HLFFN are concatenated and fed as input to a Fully Connected (FC) layer and a softmax layer having 4 output classes. The concatenated high and low level feature vector is the final rich multilevel feature representation of an input patch.

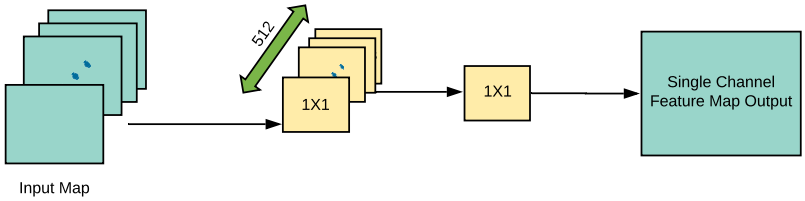

Fig. 4: The Feature Control Unit(FCU)

Training Details The two pretrained VGG19 backbone nets are fine tuned individually, independent of each other and other networks—— one on Vahadane stain normalized patch dataset, and the other on Macenko stain normalized patch dataset. After fine-tuning, the final weights of both the nets are frozen for later use. The FCUs and the SFFN network are trained jointly—— the Vahadane and Macenko stain normalized versions of an input patch are fed to the corresponding backbone networks and the information flows via the FCUs to the SFFN, which are trained using an integrated loss function. When these nets are trained with this integrated objective, weights of only the FCUs and the SFFN are updated, and those of the backbone nets are not updated by back-propagation. The integrated loss function, inspired by [7], takes the predictions of the backbone networks, into account. This is done to incorporate predictions by considering only Vahadane [16] or Macenko [9] stain normalized inputs and

predictions using a rich feature combination of both, and thereby aiding the feature fusion mechanism of the SFFN. The integrated loss function is formally expressed as,

$$L_{Intg} = \sum_{i=1}^{3} \alpha_i L_i \tag{1}$$

where where L_i and α_i are the loss and tuning weight of the i^{th} model respectively. The three models here, are the backbone network trained on Macenko [9] stain normalized patches($i = 1$), the backbone network trained on Vahadane [16] stain normalized patches ($i = 2$) and $i = 3$ corresponds to the SFFN and FCU trained in parallel. We empirically set the hyperparameters α_1, α_2, α_3 to 1, 1 and 0.5 respectively. Each loss function L_i is a cross entropy loss which is defined as:

$$L_i = -\sum_{j=1}^{k} y_j log(\hat{y}_{i,j}) \tag{2}$$

where k is the number of classes, which in our case is 4 (Benign, Normal, Insitu Carcinoma and Invasive Carcinoma). y_j is the j^{th} value of the ground truth label, $\hat{y}_{i,j}$ is the j^{th} value of softmax output of network i.

$$\hat{y}_{i,j} = g_s(l_{i,j}) \tag{3}$$

where $l_{i,j}$ is the j^{th} logit value of network i and $g_s(.)$ is the softmax activation function.

Both the backbone CNNs and joint SFFN and FCU networks are trained using the Stochastic Gradient Descent Optimizer (SGD) optimizer.

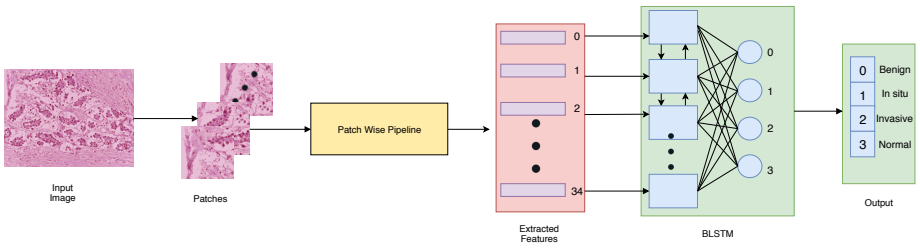

Fig. 5: The image wise pipeline

3.4 Image wise classification

After classifying the constituent patches of a high resolution histopathology image, the next problem is to integrate the patch level features or predictions,

to obtain the output class of the image. Most previous methods use majority voting or a SVM classifier for that purpose. But the problem that arises by using those methods, is the inability to maintain the long and short term associations between the patches of an image, and the inability to incorporate contextual information of neighbouring patches. Integration of the results of individual patches are thus computed using a bi-directional LSTM. The BLSTM helps retain contextual information by processing from both left-to-right and right-to-left, thereby taking into account past, as well as future context for every patch. We concatenate the multilevel feature vector output from the SFFN, as input to a BLSTM. Thus each timestep of the LSTM corresponds to a patch of the original image. A four node fully connected layer with softmax activation, is connected to the end of the network, to output the class of the entire image. The BLSTM network is trained with Adadelta optimizer.

4 Experiments

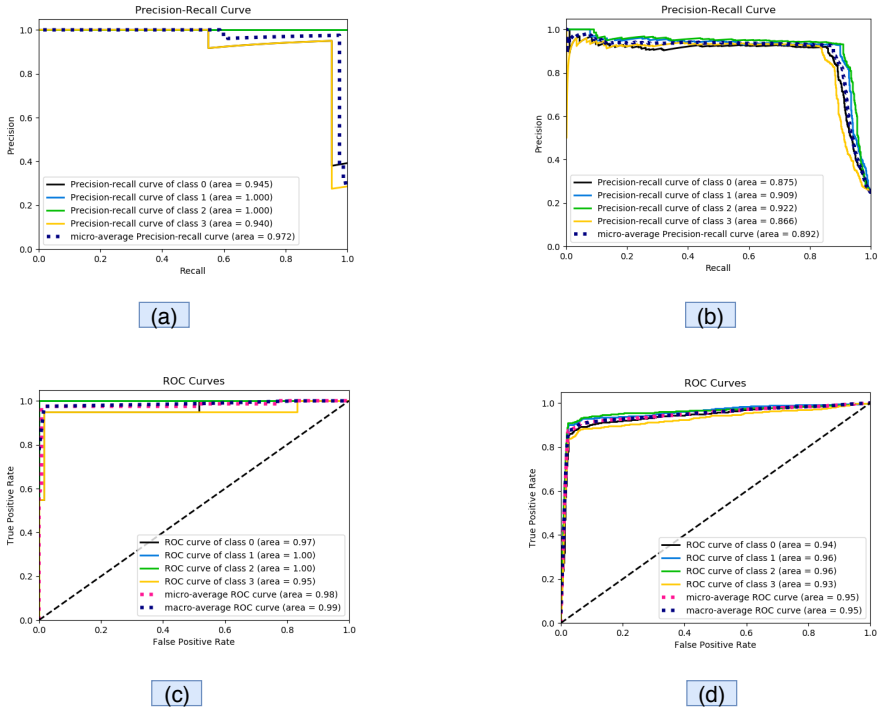

Fig. 6: Precision-Recall Curves for a)Image Wise and b)Patch-Wise classification and ROC curves for c)Image Wise and d)Patch-Wise classification for the four classes.0:Benign, 1:Insitu, 2:Invasive, 3:Normal

Following the standard practice, the ICIAR 2018 [2] data set is split into three parts for training, validation and testing purposes. 70%, 10% and 20% of the images are used for training, validation and testing

Table 1: Comparison of the 4-class classification accuracy of the proposed model with baseline models. M-VGG19 and V-VGG19 corresponds to the backbone VGG-19 nets finetuned on Macenko and Vahadane stain normalized patch datasets respectively.

Model		**Accuracy (%)**	
Patch wise	*Image wise*	*Patch wise*	*Image wise*
M-VGG19	SVM	84.50	90
V-VGG19	SVM	85.70	91.25
M-VGG19	Majority Vote	84.50	88.75
V-VGG19	Majority Vote	85.70	90
M-VGG19	BLSTM	84.50	92.50
V-VGG19	BLSTM	85.70	93.75
Proposed		87.75	97.50

respectively. The classification performance of the entire model is evaluated using metrics like accuracy, precision, sensitivity, specificity. The 4-class patch and image level classification accuracies are 87.75% and 97.5% respectively. The 2-class patch and image level classification accuracies are 96% and 98.75% respectively. 2-class classification entails in classifying a patch as carcinoma (insitu, invasive) or non-carcinoma (benign,normal). To evaluate the effectiveness of hierarchical feature fusion of two stain normalized versions of an input patch over the individual backbone networks, and to evaluate the efficacy of BLSTM over SVM or majority voting for image wise classification, we compare our final model with some baselines. Figure 7 shows the confusion matrices for image and patch wise classifications while Figure 6 shows the precision recall curves for the same. From Table 1, we can see that the proposed model incorporating high level and low level features of both the stain normalized patches, perform better than the models using a single stain normalized patch. Also it can be seen that, using the BLSTM in the image wise pipeline in Figure 5 gives better classification performance compared to SVM and Majority Voting.Table 2 provides us with image-wise and patch-wise metrics of 4-class classifications while,from Table 3, we can see that our proposed model outperforms other state of the art methods, both for four-class and two-class classification.

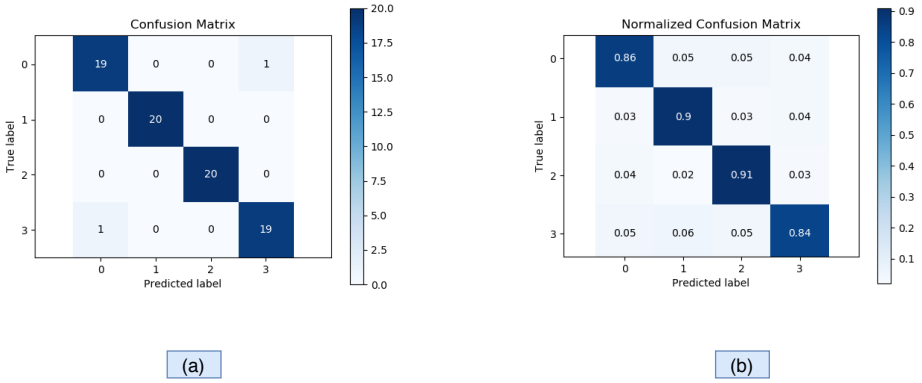

Fig. 7: Confusion Matrix for a)image wise and b)patch-wise classification. 0:Benign, 1:Insitu, 2:Invasive, 3:Normal

Table 2: Image Wise and Patch Wise metrics of 4 class classification

Metric Type	**Metrics**	**Classes**				**Avg**
		Benign	**InSitu**	**Invasive**	**Normal**	
Patch Wise	**Precision**	87.88	87.37	87.62	88.15	87.75
	Sensitivity	86	90	91	84	87.75
	Specificity	96.04	95.66	95.71	96.23	95.91
	F1 Score	86.93	88.66	89.27	86.02	87.72
Image Wise	**Precision**	95	100	100	95	97.5
	Sensitivity	95	100	100	95	97.5
	Specificity	98.33	100	100	98.33	99.16
	F1 Score	86.995	100	100	95	97.5

Table 3: Comparison of proposed method with some state of the art methods

Method	**Dataset Used**	**Number of Classes**	**Patch Level Accuracy(%)**	**Image Level Accuracy(%)**
Araujo et al. [1]	Bioimaging 2015	4	66.7	77.8
Araujo et al. [1]	Bioimaging 2015	2	77.6	83.3
Rakhlin et al. [11]	ICIAR 2018	4	-	87.5
Rakhlin et al. [11]	ICIAR 2018	2	-	93.8
Vang et al. [17]	ICIAR 2018	4	-	87.5
Golatkar et al. [5]	ICIAR 2018	4	79	85
Golatkar et al. [5]	ICIAR 2018	2	-	93
Roy et al. [12]	ICIAR 2018	4	77.4	90
Roy et al. [12]	ICIAR 2018	2	84.7	92.5
Nazeri et al. [10]	ICIAR 2018	4	-	95
Wang et al. [18]	ICIAR 2018	4	-	91
Proposed Method	ICIAR 2018	4	87.75	97.50
Proposed Method	ICIAR 2018	2	96	98.75

5 Conclusion

In this study, we proposed a novel architecture based on spatial fusion of features of two different stain normalisations of an input 512×512 patch. To use the long term and short term contextual information between patches for classifying the entire high resolution image, we extract a feature representation from every patch and feed it as input at every time step of a BLSTM network. We demonstrate that, incorporating features of two differently stain normalized patches, give better classification results than CNNs trained on any one of the stain normalized patches. For image level classification, using BLSTM gives better results compared to combining patch wise results with Majority Voting and SVM. In this paper, we also present a novel architectural component, namely the Feature Control Unit (FCU), which regulates the nature of features flowing into the SFFN network. Our method achieved a 87.75% and 97.5% accuracy on 4-class patch and image wise classification respectively, thereby outperforming other state of the art methods. Despite our model achieved good results, the most conspicuous caveat of it is that the design is a bit complex hence demanding more training and prediction time. The other one is that our model has a two stage architecture——one for patch wise classification and the other for image wise classification, thus the output of a high resolution image can not be obtained in a single forward pass. Although these limitations are not critical as our problem statement does not demand a real time performance, they can be overcome by designing efficient end to end model architectures, where an entire high resolution image can be fed to the network. For future work, we will work on designing these end to end models, to overcome the above caveats.

References

1. Araújo, T., Aresta, G., Castro, E., Rouco, J., Aguiar, P., Eloy, C., Polónia, A., Campilho, A.: Classification of breast cancer histology images using convolutional neural networks. PloS one **12**(6), e0177544 (2017)
2. Aresta, G., Araújo, T., Kwok, S., Chennamsetty, S.S., Safwan, M., Alex, V., Marami, B., Prastawa, M., Chan, M., Donovan, M., et al.: Bach: Grand challenge on breast cancer histology images. Medical image analysis (2019)
3. Deng, J., Dong, W., Socher, R., Li, L.J., Li, K., Fei-Fei, L.: Imagenet: A large-scale hierarchical image database. In: 2009 IEEE conference on computer vision and pattern recognition. pp. 248–255. Ieee (2009)
4. Glorot, X., Bordes, A., Bengio, Y.: Deep sparse rectifier neural networks. In: Proceedings of the fourteenth international conference on artificial intelligence and statistics. pp. 315–323 (2011)
5. Golatkar, A., Anand, D., Sethi, A.: Classification of breast cancer histology using deep learning. In: International Conference Image Analysis and Recognition. pp. 837–844. Springer (2018)
6. Hochreiter, S., Schmidhuber, J.: Long short-term memory. Neural computation **9**(8), 1735–1780 (1997)
7. Jung, H., Lee, S., Yim, J., Park, S., Kim, J.: Joint fine-tuning in deep neural networks for facial expression recognition. In: Proceedings of the IEEE international conference on computer vision. pp. 2983–2991 (2015)

8. Lin, M., Chen, Q., Yan, S.: Network in network. arXiv preprint arXiv:1312.4400 (2013)
9. Macenko, M., Niethammer, M., Marron, J.S., Borland, D., Woosley, J.T., Guan, X., Schmitt, C., Thomas, N.E.: A method for normalizing histology slides for quantitative analysis. In: 2009 IEEE International Symposium on Biomedical Imaging: From Nano to Macro. pp. 1107–1110. IEEE (2009)
10. Nazeri, K., Aminpour, A., Ebrahimi, M.: Two-stage convolutional neural network for breast cancer histology image classification. In: International Conference Image Analysis and Recognition. pp. 717–726. Springer (2018)
11. Rakhlin, A., Shvets, A., Iglovikov, V., Kalinin, A.A.: Deep convolutional neural networks for breast cancer histology image analysis. In: International Conference Image Analysis and Recognition. pp. 737–744. Springer (2018)
12. Roy, K., Banik, D., Bhattacharjee, D., Nasipuri, M.: Patch-based system for classification of breast histology images using deep learning. Computerized Medical Imaging and Graphics **71**, 90–103 (2019)
13. Simonyan, K., Zisserman, A.: Very deep convolutional networks for large-scale image recognition. arXiv preprint arXiv:1409.1556 (2014)
14. Spanhol, F.A., Oliveira, L.S., Petitjean, C., Heutte, L.: A dataset for breast cancer histopathological image classification. IEEE Transactions on Biomedical Engineering **63**(7), 1455–1462 (2015)
15. Szegedy, C., Liu, W., Jia, Y., Sermanet, P., Reed, S., Anguelov, D., Erhan, D., Vanhoucke, V., Rabinovich, A., et al.: Going deeper with convolutions. arxiv 2014. arXiv preprint arXiv:1409.4842 **1409** (2014)
16. Vahadane, A., Peng, T., Sethi, A., Albarqouni, S., Wang, L., Baust, M., Steiger, K., Schlitter, A.M., Esposito, I., Navab, N.: Structure-preserving color normalization and sparse stain separation for histological images. IEEE transactions on medical imaging **35**(8), 1962–1971 (2016)
17. Vang, Y.S., Chen, Z., Xie, X.: Deep learning framework for multi-class breast cancer histology image classification. In: International Conference Image Analysis and Recognition. pp. 914–922. Springer (2018)
18. Wang, Y., Sun, L., Ma, K., Fang, J.: Breast cancer microscope image classification based on cnn with image deformation. In: International Conference Image Analysis and Recognition. pp. 845–852. Springer (2018)